Electronic Supplementary Information

Thermo-responsive polymer catalysts for polyester recycling processes: Switching from homogeneous catalysis to heterogeneous separations

Victor Daniel Lechuga-Islas, [a,b]* Dulce M. Sánchez-Cerrillo, [a] Steffi Stumpf, [a,c] Ramiro Guerrero-Santos, [b]* Ulrich S. Schubert, [a,c] and Carlos Guerrero-Sánchez [a,b]*

[a] Laboratory of Organic and Macromolecular Chemistry (IOMC), Friedrich Schiller University Jena, Humboldtstrasse 10, 07743 Jena, Germany.

[b] Centro de Investigación en Química Aplicada (CIQA), Department of Macromolecular Chemistry and Nanomaterials, Enrique Reyna H. 140, Saltillo, 25100, Mexico.

[c] Jena Center for Soft Matter (JCSM), Friedrich Schiller University Jena, Philosophenweg 7, 07743 Jena, Germany.

Email: carlos.guerrero.sanchez@uni-jena.de

Contents

Materials and methods 2

General Procedure for PET glycolysis 5

Procedure of polymer catalyst reusability 6

Characterization methods 7

Figures and Tables SI 9

Solution behavior of of [PIL]Cl and [PIL]Zn_mCl_n 11

References 23

Materials and methods

Synthesis of Poly(ionic liquid)s (PILs): 1-Methyl imidazole (99%), 1-butyl imidazole (98%), and the monomer 4-vinylbenzyl chloride (90%) were acquired from TCI Chemicals. The thermal initiator 4,4'-Azobis(4-cyanovaleric acid) (ACVA, 75%) and the internal reference 1,3,5-trioxane (≥99%) were acquired from Sigma Aldrich and used as received. 4-Vinylbenzyl chloride was treated with inhibitor removers before use. The chain transfer agent 4-Cyano-4-[(dodecylsulfanylthiocarbonyl)sulfanyl]pentanoic acid (CDTPA, ≥97%) was acquired from STREM Chemicals and used as received. The salts used for anion exchange reactions ($ZnCl_2$ (98%), $FeCl_3$ (99%), and $CoCl_2$ (98%) were acquired from Sigma Aldrich and used as received. Solvents: dimethyl sulfoxide (DMSO, ≥99.5%) ethylene glycol (EG, 99%), glycerol (99%), and 1,3-propanediol (98%) were acquired from Aldrich and used without further purification.

Polyethylene terephthalate (PET) glycolysis: PET flakes (A ~ 2 mm^2) were obtained from transparent post-consumer PET bottles. Before the glycolysis procedure, the PET flakes were washed with H_2O and methanol (three times each). Next, the PET flakes were filtered and dried in a vacuum oven at 90 °C for 12 h.

Synthesis of monomers 1-methyl-3-(4'-vinylbenzyl)-1H-imidazol-3-ium chloride ([BVBIM]Cl) and 1-butyl-3-(4'-vinylbenzyl)-1H-imidazol-3-ium chloride ([BVMIM]Cl). A slightly modified procedure from the literature was used for the synthesis of the ionic monomers.[1] Briefly, 1-butylimidazole (8.03 g, 8.5 mL, 64.6 mmol) and 4-vinylbenzyl chloride (9.75 g, 9.0 mL, 63.9 mmol) were dissolved in $CHCl_3$ (80 mL) in a 250-mL round-bottom flask. The reaction was performed by first sparging N_2 in the reaction mixture for 20 min to deplete O_2, followed by heating at reflux temperature (45 °C) for 24 h. The reaction was then stopped and cooled to r. t. Thereafter, the reaction mixture was extracted with water (3 × 30 mL), and the aqueous phase was freeze-dried to remove solvents. Finally, 12.6 g of [BVBIM]Cl (71% yield) were obtained as a colorless, highly viscous liquid. The same procedure was followed for the synthesis of [BVMIM]Cl (72% yield), using 1-methyl imidazole as reactant. The obtained monomers were characterized by Proton Nuclear Magnetic Resonance (^{1}H NMR):

- ^{1}H NMR of [BVMIM]Cl (DMSO-d_6, 300 MHz) δ = 9.51 (s, 1H, N-CH), 7.99 – 7.67 (m, 2H, CH=CH), 7.65 – 7.28 (m, 4H, ArH), 6.74 (dd, *J* = 17.7, 10.9 Hz, 1H, Ar-CH), 5.87 (dd, *J* = 17.6, 1.0 Hz, 1H, CH=CH), 5.47 (s, 2H, N-CH_2), 5.29 (dd, *J* = 10.9, 1.0 Hz, 1H, CH=CH),

3.87 (s, 3H, N-CH_3). Elemental analysis calcd (%): C, 66.52; H, 6.44; N, 11.93, Cl 15.1; found C, 64.66; H, 6.68; N, 11.65, Cl, 14.18.

^{1}H NMR of [BVBIM]Cl (DMSO-d_6, 300 MHz) δ = 9.93 (s, 1H, N-CH), 8.00 (dd, *J* = 16.2, 1.7 Hz, 2H, CH=CH), 7.62 – 7.31 (m, 4H, ArH), 6.69 (dd, *J* = 17.7, 10.9 Hz, 1H, Ar-CH), 5.82 (d, *J* = 17.7 Hz, 1H, CH=CH), 5.56 (s, 2H, N-CH_2), 5.23 (d, *J* = 10.9 Hz, 1H, CH=CH), 4.22 (t, *J* = 7.2 Hz, 2H, N-CH_2), 1.73 (p, *J* = 7.3 Hz, CH_2-CH_2), 1.18 (h, *J* = 7.4 Hz, 2H, CH_2-CH_2), 0.81 (t, *J* = 7.3 Hz, 3H, CH_2-CH_3). Elemental analysis calcd (%): C, 69.4; H, 7.65; N, 10.12, Cl 12.81; found C, 64.66; H, 7.78; N, 9.56, Cl, 12.11.

Reversible addition-fragmentation chain transfer (RAFT) polymerization: Polymerizations were performed in a commercially available automated parallel synthesizer (ASW 2000) from Chemspeed Technologies AG (Switzerland). The synthesizer was equipped with a glass reactor block consisting of 16 reaction vessels (13 mL) provided with thermal jackets connected in series through the reaction block to a heating/cooling system (Hüber, −20 to 140 °C) and vortex agitation (up to 1400 rpm). Besides, each reaction vessel was equipped with a cold-finger reflux condenser (∼5 °C). A liquid handling system composed of a needle head (NH) was used for sampling. The NH was connected to a solvent reservoir bottle (ethanol (EtOH)) for needle rinsing after each liquid transfer. Before each experiment, the reaction vessels were heated to 130 °C followed by 10 cycles of vacuum / filling with N_2 (2 min each) to deplete moisture and oxygen. After this pre-treatment, RAFT polymerizations were performed according to the procedures described in the following section.

Synthesis of poly[1-methyl-3-(4'-vinylbenzyl)-1H-imidazol-3-ium chloride] (P([BVMIM]Cl)) and poly[1-butyl-3-(4'-vinylbenzyl)-1H-imidazol-3-ium chloride] (P([BVBIM]Cl)). Scheme 1 (Main Manuscript) describes synthetic route followed to produce PILs. The RAFT polymerizations were carried out using CDTPA as a chain transfer agent, which effectively controls the polymerization of styrenic and methacrylate monomers.[1] As pointed out by Barner-Kowollik *et al*., aprotic solvents are suitable to perform the RAFT polymerization of ionic monomers;[2] thus, DMSO was used as a reaction solvent to ensure optimal dissolution of the ionic monomers and good control over polymerization (see Table SI 1 for details). A series of Cl-type PILs with variable degree of polymerization were obtained according to the corresponding CDTPA ratio. A representative synthesis procedure is as follows: a septum sealed flask was charged with the stated quantities of [BVBIM]Cl, ACVA, CDTPA, and 1,3,5-

trioxane (Table SI 1). The mixture was dispersed in DMSO and stirred until dissolution. Thereafter, the reaction mixture was charged into the reactors of the automated parallel synthesizer and degassed by sparging N_2 for 20 min. Subsequently, the reactor block was sealed under a nitrogen atmosphere and heated to 80 °C for 16 to 24 h. The onset of the polymerization was considered once the reaction temperature was reached. Monomer conversion was followed by ^{1}H NMR measurements by withdrawing aliquots from the reactor at different times (vinylic signals of the monomers at $\delta \approx 6.7$ and 5.0 ppm and reference signal of trioxane at 5.1 ppm). After the reaction time elapsed, the polymer solution was concentrated by rotatory evaporation and purified by dialysis in deionized water (48 h, r.t., membrane of 1.0 kg mol^{-1} MWCO). The final product was freeze-dried for 24 h to obtain a yellow-colored solid.

Table SI 1. Experimental details for the synthesis of P([BVMIM]Cl) (**A1** – **A4**) and P([BVBIM]Cl) (**B1** – **B2**).

Entry	[M / CTA]	Solvent [mL]	Monomer [mmol]	CDTPA [mmol]	ACVA [mmol]	Trioxane [mmol]
A1	23.02	8.0	5.0	0.217	0.043	0.710
A2	44.32	8.0	5.0	0.056	0.011	0.710
A3	123.3	25.6	16.5	0.134	0.020	2.27
A4	214.7	25.6	16.5	0.077	0.012	2.27
B1	18.0	5.40	7.2	0.40	0.080	0.60
B2	36.1	5.40	7.2	0.20	0.040	0.60

Anion exchange reactions. Series of P([BVMIM]Zn_mCl_n) and P([BVBIM]Zn_mCl_n) were obtained by reacting the corresponding PIL precursor with metal salts at elevated temperature (Scheme 1). A representative procedure is as follows: a septum sealed flask was charged with 0.150 g of P([BVBIM]Cl) and 4 mL of EtOH. Next, the mixture was stirred until complete dissolution and degassed by sparging N_2 for 20 min. The flask was then immersed in a preheated oil bath at 80 °C. After heating the mixture for 30 min, anion exchange was performed by adding a solution of $ZnCl_2$ dissolved in EtOH (10 mg mL^{-1}). Heating and stirring continued for 12 h. Upon adding the $ZnCl_2$ solution to the reaction mixture, a viscous precipitate was observed. The obtained heterogeneous mixture was purified by completing the precipitation of the polymer into acetone. Finally, the precipitate was washed three

times with 10 mL of EtOH each to remove any excess of the salt. The same procedure was followed to perform anion exchange of P([BVMIM]Cl) precursors with $ZnCl_2$, $FeCl_3$, and $CoCl_2$. The obtained solid was dried until constant weight in a vacuum oven at 40 °C. The ratio of metallic salt was calculated according to eq. 1:

$$R = \frac{n_{MCl_n}}{n_{MCl_n} + n_{[BVRIM]Cl}} \qquad \text{eq. 1}$$

Where n_{MCl_n} represents moles of metal salt and $n_{[BVRIM]Cl}$ represents moles of the corresponding polymerized monomer [BVMIM]Cl or [BVBIM]Cl (estimated by ^{1}H NMR).

General Procedure for PET glycolysis

The catalytic performance of the obtained polymer catalysts was evaluated in glycolysis experiments using a FORMAX platform from Chemspeed Technologies AG (Switzerland). As shown in Figure SI 10, the platform is equipped with a formulation block composed of six reactors (V = 100 mL), each with an independent thermal jacket, a thermocouple, mechanical stirring (anchor, disk-type, or disperser disc), and a reflux condenser (Figure SI 10A and inset). Each reactor can be independently heated up to 250 °C or cooled down with a heating/cooling system (Hüber cryostat -20 to 140 °C). For transferring liquids and solid materials, a 4-needle head (4-NH) (Figure SI 10B) and gravimetric dispensing units (Figure SI 10D) were available, respectively. The 4-NH was connected to a block of 4 syringe pumps (V = 1 and 10 mL, Figure SI 10C) and a solvent reservoir bottle (EtOH) for needle rinsing after each liquid transfer.

Sets of up to 6 glycolysis reactions were performed in open reactors. For this purpose, the corresponding amount of polymer catalyst and 35 mL of EG were charged into the reactors of the formulation block. Thereafter, each reactor vessel was heated to 180 °C (jacket set point = 215 °C) with a stirring speed of 500 rpm. After reaching thermal equilibrium (*ca.* 20 min), the glycolysis reaction was started by adding the corresponding amount of post-consumer PET flakes (weight ratio PET:EG = 1:4). The onset of the reaction was set upon adding PET flakes. Then, heating and stirring continued for 4 h. After the reaction time elapsed, the mixture was cooled down to 50 °C (via a Hüber cryostat). Then, 100 mL of deionized water (T = 60 °C) were added to the final mixture to wash and remove unreacted

PET flakes, oligomers, and hydrophobic impurities from the product. The final mixture was heated (T = 80 °C for *ca.* 20 min) to solubilize the maximum amount of produced monomer (Bis(2-Hydroxyethyl) terephthalate (BHET)). Finally, the aqueous mixture was filtered, and insoluble by-products (unreacted PET, oligomers, and hydrophobic impurities) were washed three times with an excess of water (3 × 30 mL). The mixture of by-products was collected, dried at 120 °C for 72 h, and weighed to estimate the conversion of PET by eq. 2:

$$Conversion\ of\ PET = \frac{W_0 - W_1}{W_0} \times 100\% \qquad \text{eq. 2}$$

Where W_0 represents the initial mass of PET and W_1 represents the mass of unreacted PET and oligomers. The collected aqueous solution was concentrated to *ca.* 100 mL by vacuum evaporation at 50 °C.

The concentrated filtrate was stored at 4 °C for 24 h for crystallization. Next, white crystalline flakes formed from the solution, which were filtered under vacuum. The recovered crystalline product was washed with water (3 × 30 mL), dried at 80 °C for 48 h, and characterized as BHET (Figure SI 11). The selectivity of BHET was estimated gravimetrically by eq. 3:

$$Selectivity\ of\ BHET = \frac{n_{BHET}}{n_{f,PET}} \times 100\% \qquad \text{eq. 3}$$

Where n_{BHET} represents the moles of BHET and $n_{f,PET}$ represents the moles of depolymerized PET. The obtained monomer was characterized by FTIR and ^{1}H NMR (Figure SI 11).

After BHET purification, the remaining mixture, containing EG, water and polymer catalyst, was concentrated by vacuum evaporation at 55 °C to remove water and yield a final solution of polymer catalyst/EG.

Procedure of polymer catalyst reusability

The reusability of the polymer catalysts was examined using the final mixture of polymer catalyst/EG as the catalyst to perform new cycles of PET glycolysis. To this end, the amount of EG used in the new glycolysis reaction was subtracted from the volume of polymer catalyst/EG solution. Besides that, the new glycolysis cycles were performed following the procedure described before. In this way, the conversion of PET and selectivity of BHET were

estimated for up to 5 depolymerization cycles (i.e., catalyst reutilization investigations). The screening of halometallate PILs as catalyst for the glycolysis of PET was performed at a lower scale in septum-sealed flasks following the same procedure described previously.

Characterization methods

^{1}H NMR spectra were recorded at r. t. on a Bruker Avance 300 MHz spectrometer using dimethyl sulfoxide (DMSO-d_6) as solvent. Chemical shifts are given in ppm. The monomer to polymer conversion was determined by comparing the integration resonance signal of the vinylic protons of the monomers and the internal standard (1,3,5-trioxane).

The number average molar mass (M_n) and molar mass distribution ($Đ$) of the obtained (co)polymers were estimated using a Jasco system equipped with a PU-980 pump, an UV-975 detector, a RI-930 detector, and a PSS NOVEMA-MAX/100/100 Å columns, 5 µm, at 30 °C, with an aqueous solution of trifluoroacetic acid (TFA, 0.3%) and NaCl 0.1 M [pH < 2] as eluent at a flow rate of 1 mL min^{-1}. The system was calibrated with 2-polyvinyl pyridine (P2VP) standards (M_p = 1,300 to 81,000 g mol^{-1}; American Polymer Standards Corp., Mentor, OH, USA).

Raman spectra were recorded using a Senterra Raman microscope (Bruker Optics, Ettlingen, Germany) for depth-resolved measurements. A diode laser (532 nm, 50 mW) was used as an excitation source. The excitation beam and the Raman backscattering radiation were guided through a 50-X objective, and a CCD detector was used for signal collection. A typical integration time for recording the Raman spectra at high resolution mode was 90 s on average. The spectral resolution was 4 cm^{-1} in the range from 75 to 1535 cm^{-1}. This spectral region was chosen because the most intense Raman bands of halometallate anions were located here.[2]

Fourier transform infrared spectroscopy (FTIR) measurements were performed using a Nicolet IS-10 FTIR instrument provided with an attenuated total reflectance (ATR) accessory.

Thermogravimetric analysis (TGA) experiments were carried out under nitrogen atmosphere with a heating rate of 10 K min^{-1} on a Netzsch TG 209 F1 Iris (Selb, Germany). Isothermal analysis was also carried out using the thermogravimetric balance. A sample of P([BVBIM]Zn_mCl_n) (derived from precursor **A2**, Table 1) was heated from 20 °C to 190 °C at

20 °C min^{-1} then maintained at 190 °C for 10 h. The entire process was carried out under a flow of air.

Differential scanning calorimetry (DSC) was measured on a Netzsch DSC 204 F1 Phoenix instrument (Selb, Germany) under a nitrogen atmosphere with a heating rate of 20 K min^{-1} (first and second heating cycles) and 10 K min^{-1} (third heating cycle).

The general sample pre-treatment for the analysis of chlorozincate PILs ([PIL]Zn_mCl_n) in solution was as follows: First, the purified polymer was mixed with the corresponding solvent and heated (T = 90 °C) in an ultrasonic bath for 30 minutes to enhance the dispersion of the polymer. After reaching a clear homogeneous solution, the solution was immediately passed through a 0.4 μm Nylon filter to remove insoluble solids. Next, the polymer solution was cooled down to r. t. for light transmission, Dynamic Light Scattering (DLS) and Scanning Electron Microscopy (SEM) studies.

Transmission measurements were performed on an Avantium Crystal 16 platform (Technobis Crystallization Systems, Netherlands) composed of 16 wells designed to hold 2-mL vials and equipped with an on-line turbidity (light transmission intensity) sensor. Each well is equipped with magnetic stirring at a fixed speed. The system is divided into four zones, with four wells each that can be independently heated or cooled. The polymer solutions (1 wt. %) were subjected to three heating-cooling cycles in the temperature range from 0 to 90 °C at a rate of 1 °C min^{-1} and a stirring speed of 500 rpm. The cloud point (T_{CP}) of the polymer solutions was recorded when the transmission signal of the apparatus reached 50%.

DLS measurements were performed on a Zetasizer Nano ZS instrument (Malvern Instruments, Germany). 3 $\times$ 30 s runs were carried out in a different temperature range (according to the T_{CP} of each sample) with an equilibration time of 180 s between each measurement (performed in triplicate). The counts were detected at an angle of 173° (λ = 633 nm). The mean particle size was approximated as the effective diameter (Z-average) and the width of the distribution as the particle polydispersity index (PDI) obtained by the cumulant method assuming spherical shapes.

Polymer nanoparticles images were acquired using a Sigma VP Field Emission Scanning Electron Microscope equipped with an Everhart-Thornley SE detector (Carl Zeiss AG,

Germany), and using an accelerating voltage of 6 kV. SEM samples were prepared by casting a drop of a polymer solution onto a silicon wafer. Thereafter, the solvent was evaporated by carefully applying a flux of air for at least 24 h. Before SEM analysis, the obtained films were coated with a thin layer of platinum via sputter coating (CCU-010 HV, Safematic, Switzerland). The average diameter was determined by particle size analysis in ImageJ software and by Gauss fitting function using the software package Origin.

SEM images of unreacted PET obtained from glycolysis experiments were recorded using a TOPCON SM-510 (TopCon, Japan) SEM equipped with an Energy-dispersive X-ray spectrometer (EDX) at an acceleration voltage of 15 kV. Prior to SEM analysis, the sample was ground to fine powder with a mortar and coated with gold films.

Figures and Tables SI

Synthesis and fundamental characterization of $[PIL]Zn_mCl_n$

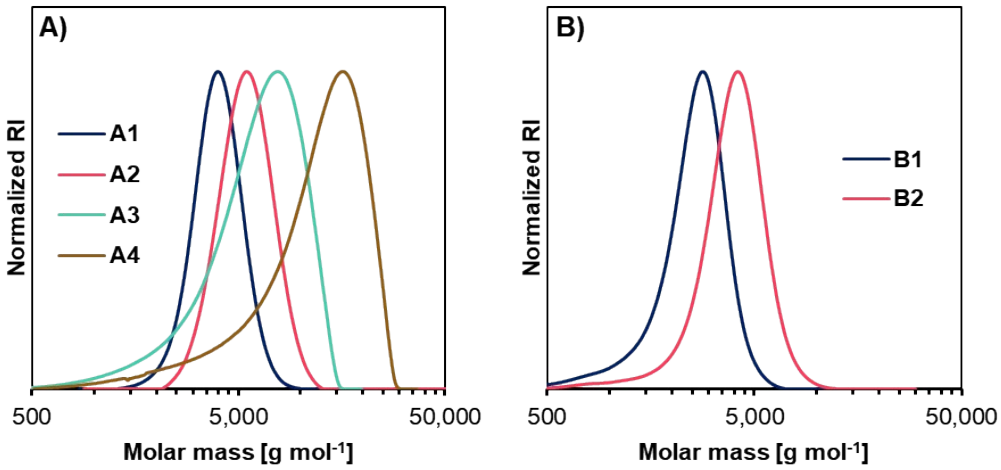

Figure SI 1. SEC traces of P([BVMIM]Cl) (**A1 – A4**) and P([BVBIM]Cl) (**B1 – B2**).

The aqueous SEC system was selected considering the solubility of the copolymers and the polyelectrolyte effect, which describes the different degrees of dissociation of polyelectrolytes due to the charges along the polymer chain. Therefore, to decrease this effect, the well-established system for polyethylene imines (PEI) was used (CF_3COOH/NaCl in aqueous solution).[3] Such a system allowed us to determine the relatively narrow dispersity of the synthesized polymers. However as briefly discussed in the Main Manuscript, stationary phases and eluent systems (pK, pH and salt concentration) in SEC, could significantly change the coil expansion of the polyelectrolyte and therefore the molar mass

estimation. Future experimentations are planned to explore such effects considering also other variables reported in this manuscript (e.g., anion exchange, anion speciation).

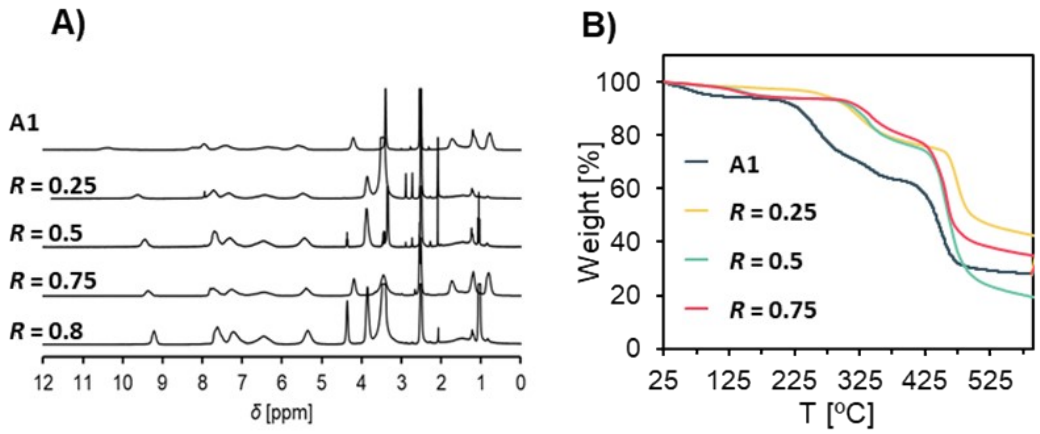

Figure SI 2. A) ^{1}H NMR spectra and B) TGA curves of P([BVBIM]Cl) (**A1**) and its anion-exchanged chlorozincate derivatives.

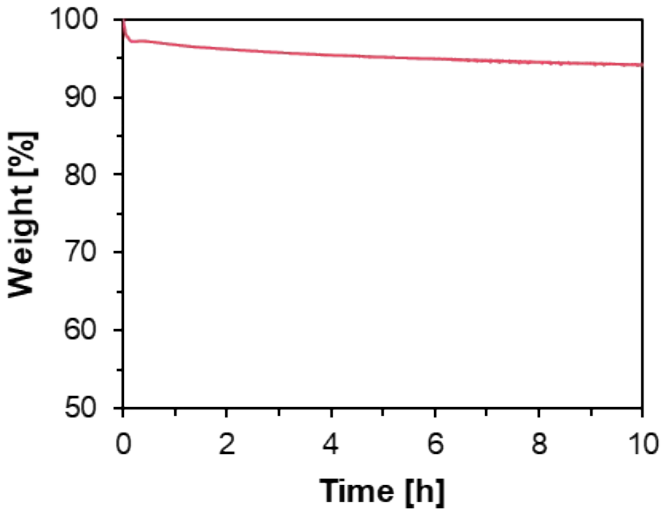

Figure SI 3. Isothermal TGA traces (190 °C) for P([BVBIM]Zn_mCl_n) derived from precursor **A2**, (Table 1, Main Manuscript).[a)]

[a)] The initial weight loss profile (~2.2 wt%, after ca. 0.25 h) could be attributed to end group loss at 190 °C, through a mechanism believed to involve homolysis of the trithiocarbonylthio RAFT agent and subsequent depropagation.[4]

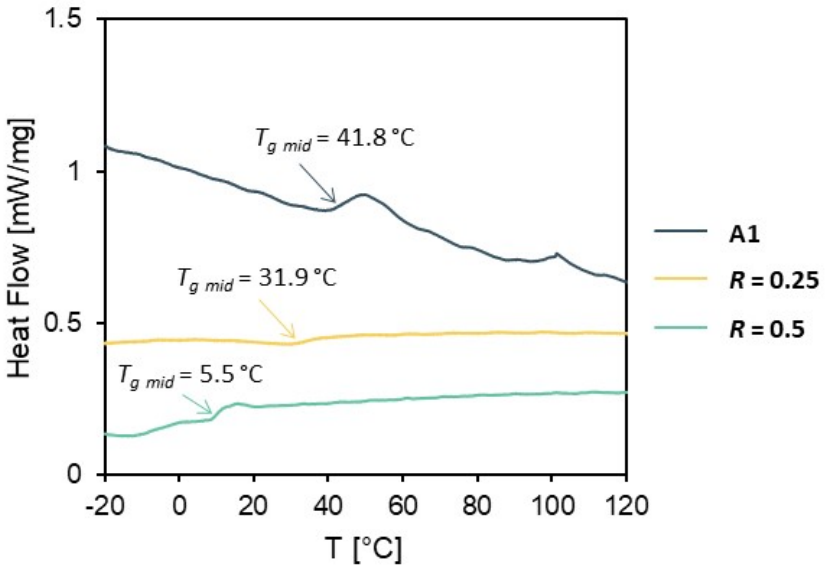

Figure SI 4. DSC thermograms of P([BVBIM]Cl) (**A1**) and its P([BVBIM]Zn_mCl_n) derivatives. [a)]

[a)] DSC thermogram of sample **A1** could be described as a complex transition, involving multiples processes, *e.g.*, melting, crystallization or relaxation enthalpy, which caused the T_g to resemble a melting peak. This could be related to the storage conditions and physical aging of the sample in its glassy state.[5,6] For more details on this complex process the reader is referred to Refs. [6–8]

Solution behavior of of [PIL]Cl and [PIL]Zn_mCl_n

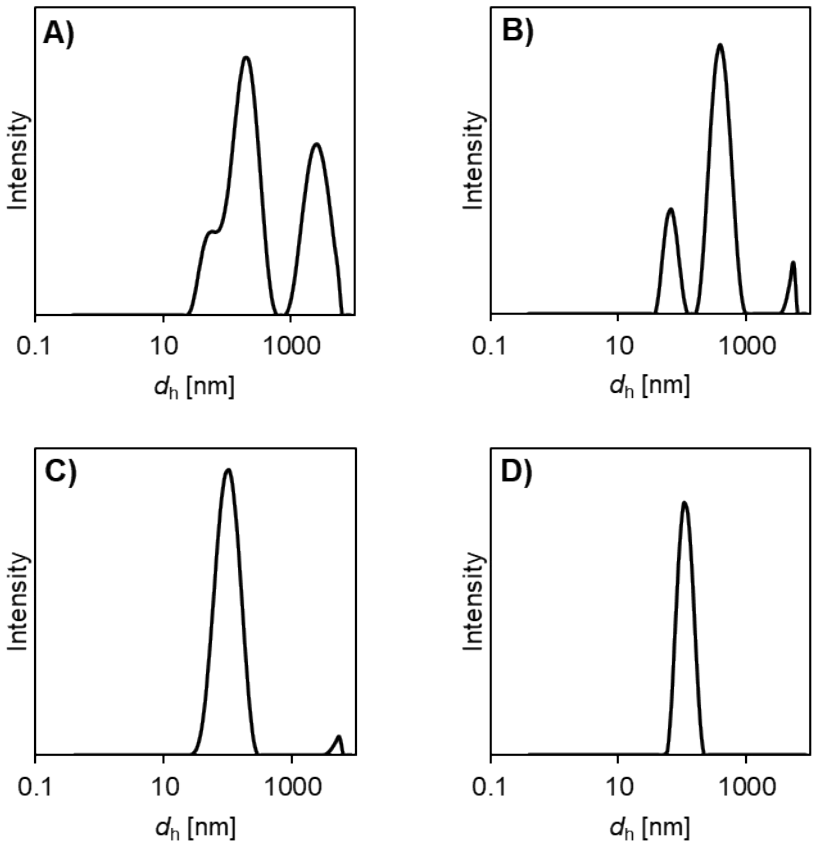

Figure SI 5. Plots of the d_h (nm) of solutions of P([BVMIM]Zn_mCl_n) (entries 3 - 6, Table 2, Main Manuscript) in EG (5 mg mL^{-1}) as a function of the *R* values of $ZnCl_2$: A) *R* = 0.1, B) *R* = 0.25, C) *R* = 0.5, and D) *R* = 0.75.

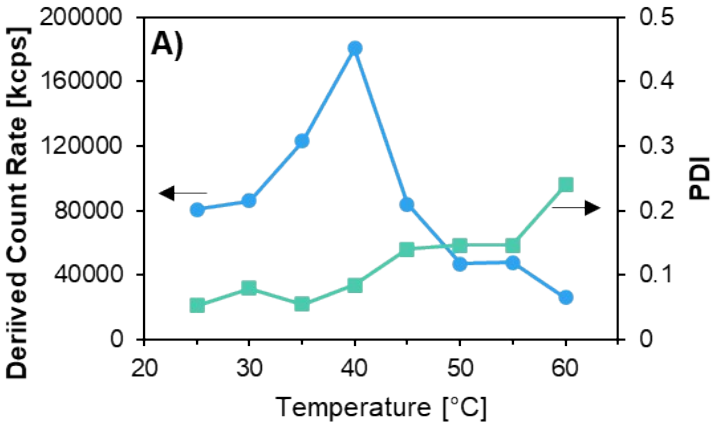

Figure SI 6. Plots of the A) derived count rate and PDI as a function of temperature, recorded by DLS, of a solution of P([BVMIM]Zn_mCl_n) in EG (**A2**, *R* = 0.75, Table 2, Main Manuscript).

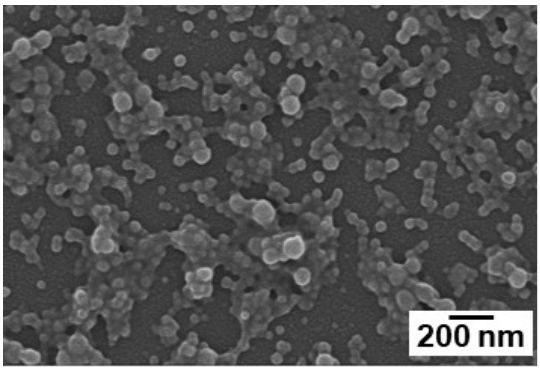

Figure SI 7. SEM image of polymeric nanoparticles after casting a solution of P([BVMIM]Zn_mCl_n) (**A2**, *R* = 0.75, Table 2, Main Manuscript) in EG (5 mg mL^{-1}) at r. t.

By examining the solution properties of P([BVMIM]Zn_mCl_n and P([BVBIM]Zn_mCl_n, and as briefly discussed in the Main Manuscript, we could envision several conditions to modulate the thermo-responsive of the copolymers by varying, for example, polymer concentration, molar mass and structure, solvents, among others. In this regard, For instance, we identified that a two-fold increase in polymer concentration in EG (from 10 to 20 mg mL^{-1}), promoted an increase in T_{CP} of the corresponding solution by more than 10 °C (Figure SI 7). In contrast, upon decreasing concentration to 5, 2 or 1 mg mL^{-1}, the solubility of the polymer significantly increased yielding colloidal suspensions with the so-called Tyndall effect (blue-transparent solution showing light scattering by the polymer nanoparticles), which did not show a phase transition detectable by light transmission experiments. For these latter cases DLS and SEM measurements revealed that solutions of **A2**, *R* = 0.75 with concentrations below 5 mg mL^{-1} produced the formation of particles with dispersed populations (*i.e.*, high polydispersity index (PDI) values and particle coalescence; Table SI 2 and Figure SI 8).

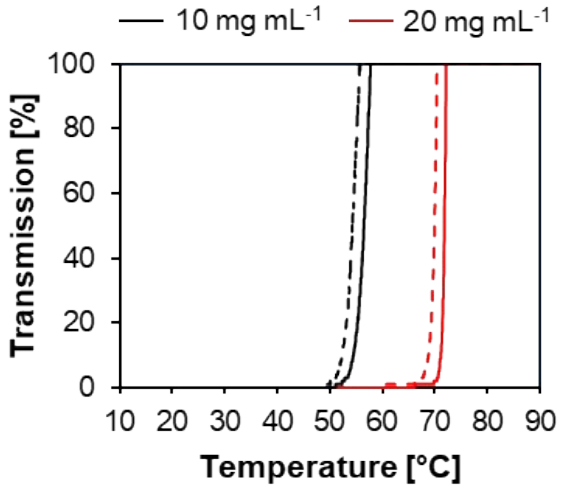

Figure SI 8. Transmission measurements of **A2**, *R* = 0.75 in EG solution (10 and 20 mg mL^{-1}); solid line: heating; dotted line: cooling.

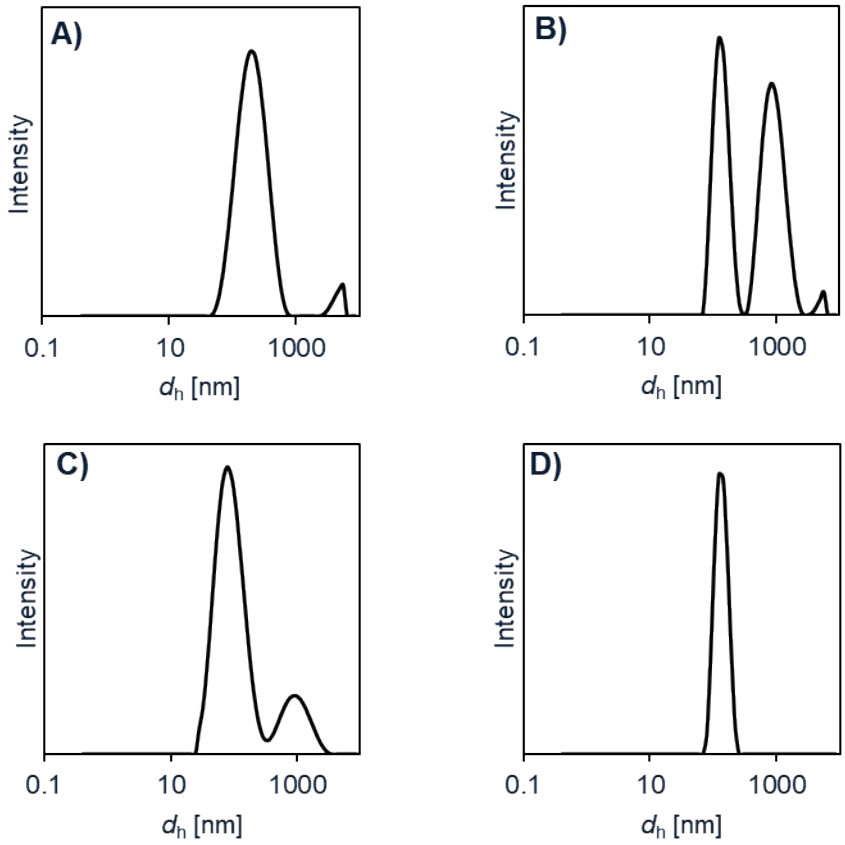

Figure SI 9. Plots of the hydrodynamic diameter (d_h, nm) of **A2**, R = 0.75 in EG (P([BVMIM]Zn_mCl_n), Table 2, Main Manuscript) as a function of polymer concentration: A) 1 mg mL^{-1}, B) 2 mg mL^{-1}, C) 5 mg mL^{-1}, and B) 10 mg mL^{-1}.

In addition, we investigated the effect of the polymer molar mass on the solution properties using the series of P([BVMIM]Zn_mCl_n) derived from precursors **A1-A4** (Table 1, Main Manuscript). In a similar trend to that reported by Aoshima *et al.*,[3] the T_{CP} of P([BVMIM]Zn_mCl_n) in EG does not exclusively depend on the degree of polymerization (DP), specifically in the low molar mass range (DP from 10 to 70, Figure SI 4B). However, we noticed that higher DP values yielded solutions of slightly lower T_{CP}, which could be ascribed to the diminished influence of the hydrophobic end groups (derived from the chain transfer agent (CTA) used during the RAFT polymerization of [PIL]Cl precursor materials) for the larger polymer chains (DP = 100, Figure SI 9A).[4]

Regarding polymer structure, we compared P([BVMIM]Zn_mCl_n) (entry 2, Table 2, Main Manuscript) and P([BVMIM]Zn_mCl_n) (entry 8, Table 2, Main Manuscript) of similar M_n, but different alkyl substituent in the imidazole group. The respective precursors and anion

exchanged derivatives showed similar solubility properties (Table 2, Main Manuscript). As determined by transmission measurements (Figure SI 9B), the recorded T_{CP} value of both derivatives showed only a small difference and a slight effect on the cooling cycles of the analyses. This variable could become more significant for longer alkyl chain or bulkier substituents, as reported elsewhere for other thermo-responsive polyelectrolytes.[5–7] This could be a topic of future investigations in this field.

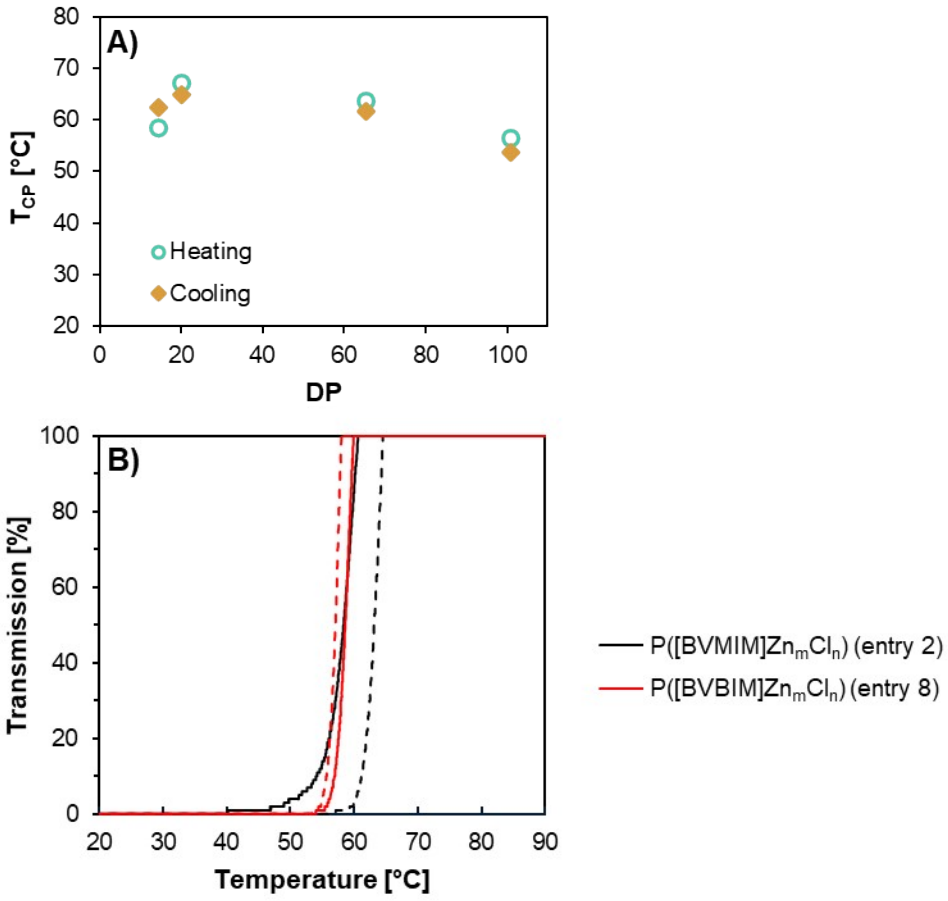

Figure SI 10. A) T_{CP} dependance on DP of solutions of P([BVMIM]Zn_mCl_n) in EG (R = 0.75, 10 mg mL^{-1}). B) Transmission measurements of [PIL]Zn_mCl_n of samples entry 2 and 8 (Table 2, Main Manuscript) in EG solutions (10 mg mL^{-1}); solid line: heating; dotted line: cooling.

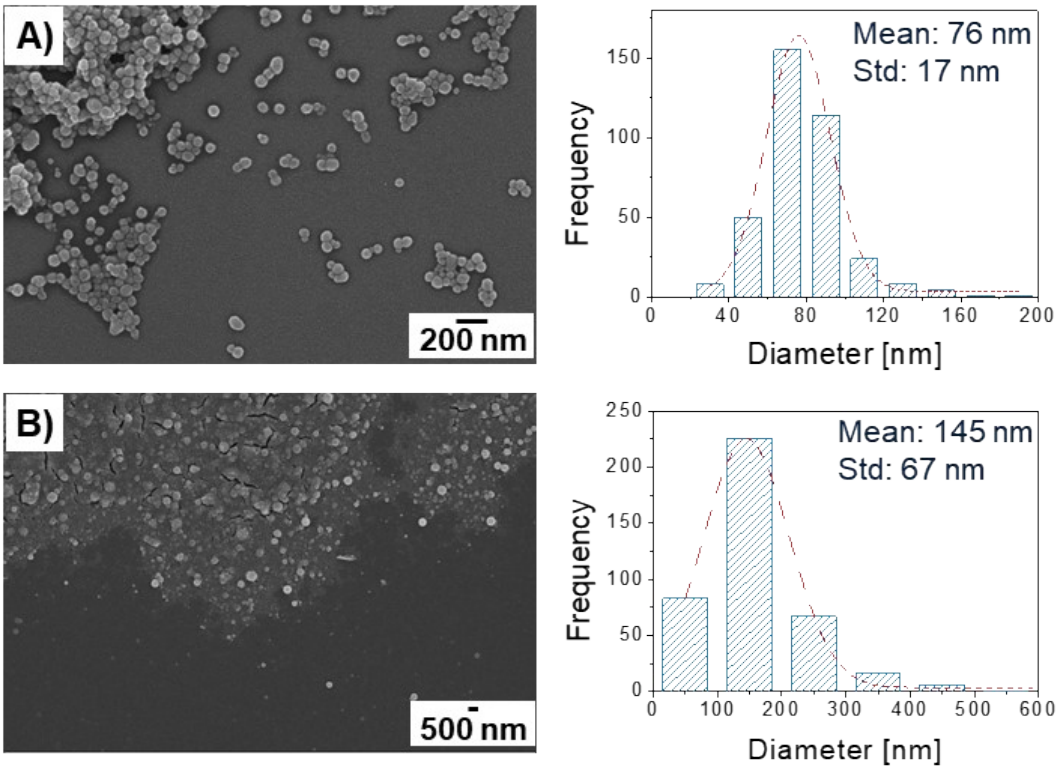

Figure SI 11. SEM images and particle size distributions of polymeric nanoparticles casted at r. t. from solutions of P([BVMIM]Zn_mCl_n) (entry 3, Table 2, Main manuscript) in different solvents: A) glycerol and B) 1,3-propanediol.

Solutions of P([BVMIM]Zn_mCl_n) (entry 3**,** Table 2, Main manuscript) in glycerol and 1,3-propanediol showed a similar thermo-responsive behavior as observed in solutions of EG. SEM images of casted solutions of P([BVMIM]Zn_mCl_n) (entry 3) in glycerol and 1,3-propanediol onto silicon wafers (Figure SI 8) also confirmed the formation of spherical nanoparticles with variable diameter depending on the utilized solvent. These supplementary results denote the capability of [PIL]Zn_mCl_n derivatives to form stable and thermo-responsive nanoparticles in glycolic solvents; therefore, extending the applicability of the proposed polymer catalysts for the glycolysis of PET in other glycolic solvents. In this context, we also observed a UCST behavior for [PIL]Zn_mCl_n derivatives in aqueous mixtures of EG (Table 2, Main Manuscript). [PIL]Zn_mCl_n derivatives with R = 0.75 (entries 2, 3 and 8) showed a UCST behavior in EG and an aqueous mixture of EG:H_2O = 95:5. Mixtures with higher concentration of H_2O vanish this phase separation phenomenon triggered by temperature. For example, for an aqueous mixture of EG:H_2O = 90:10, we only observed solutions with the Tyndall effect and no T_{CP} was detected by transmission measurements. Then, the thermo-responsive behavior completely vanished at higher H_2O ratios. This could

be ascribed to the moderate solubility of $ZnCl_2$ in H_2O. At fixed pH conditions and ionic strength, $ZnCl_2$ can be solubilized in aqueous solutions; however, an excess of water promotes the formation of zinc oxychloride and lead to precipitation.[9,10] Hence, in our [PIL]Zn_mCl_n systems, the presence of H_2O could increase the solubility of the polymer. On the other hand, the formation of zinc oxychloride species in pure water solutions might hinder the formation of stable nanoparticles in the medium, and consequently, influencing the solubility of the polymer.

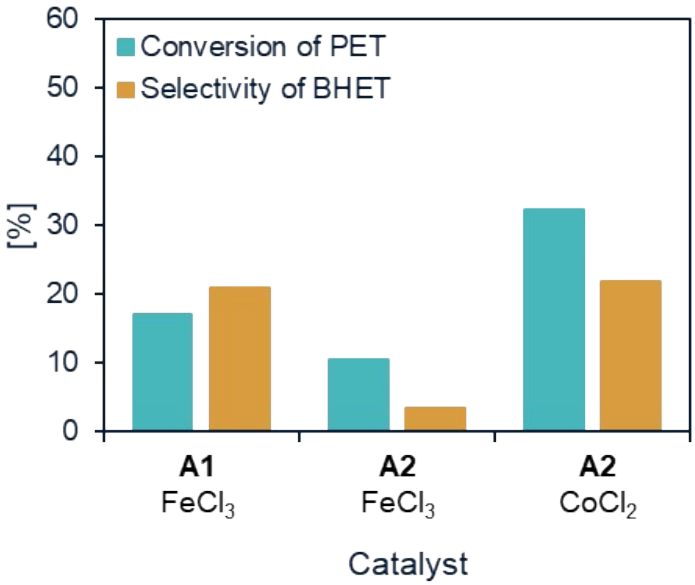

Figure SI 12. Effect of halometallate PIL derivatives of $FeCl_3$ and $CoCl_2$ (precursor and anion indicated) on the glycolysis PET and selectivity of BHET (T = 180 °C, t = 4 h).

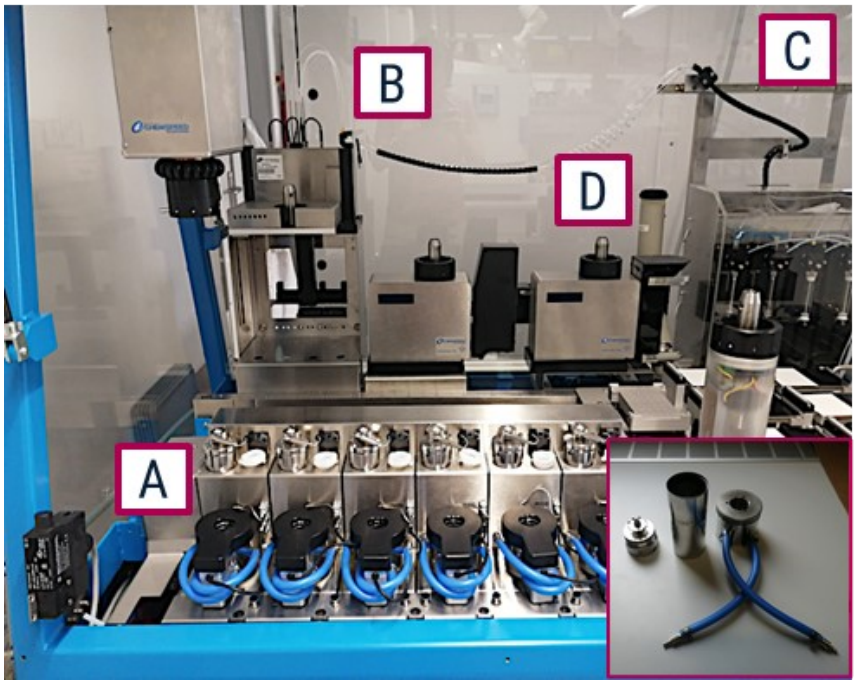

Figure SI 13. Front picture of the formulation block in the FORMAX platform. The inset shows a picture of the disassembled reactor, showing the mechanical stirrer used in this work.

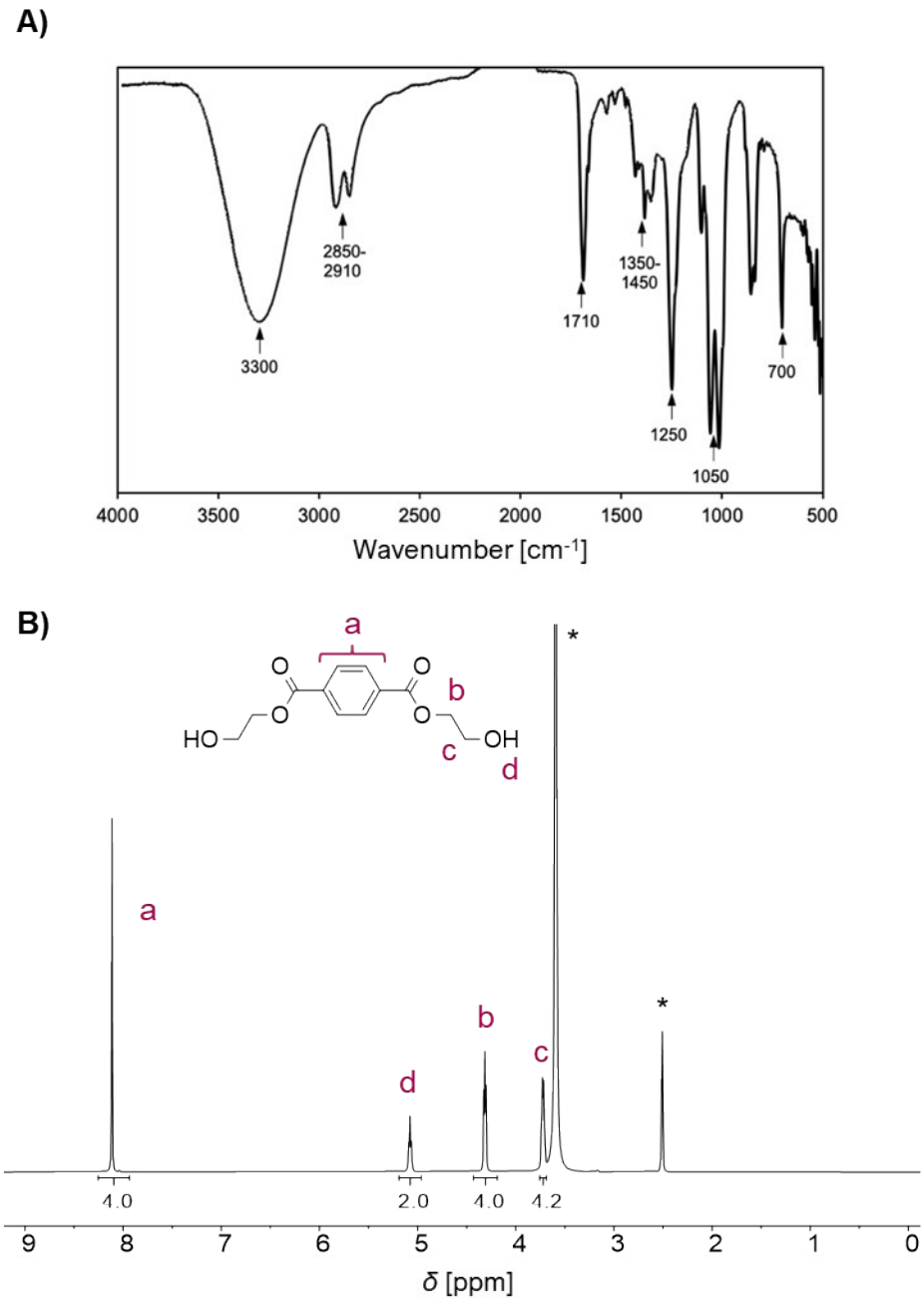

Figure SI 14. A) FTIR and B) ^{1}H NMR spectra (DMSO-d_6) of the main product of glycolysis (BHET) after purification by crystallization.

FTIR spectra of the isolated crystalline product obtained from PET glycolysis is shown in Figure SI 11A. The structure of BHET was confirmed by the -OH signals (3350 cm^{-1} and 1135 cm^{-1}) and C=O (1710 cm^{-1}) stretch bands.[11] Furthermore, signals at 2850 and 2910 cm^{-1} evidenced the C-H stretch bands from the alkyl chain. The set of signals at 1350-1450 and 700 cm^{-1} corresponds to the C=C stretch and C-H bend of the *p*-disubstitued aromatic group, respectively. The bands at 1250 and 1050 cm^{-1} were attributed to the C-O-C of the ester group and the C-O of the hydroxy group of the primary alcohol.

An exemplary ^{1}H NMR in DMSO-d_6 of the crystalline product is reproduced in Figure SI 11B. The singlet signal at δ = 7.9 ppm indicates the presence of the four aromatic protons of the *p*-substituted aromatic group. The triplet signal at δ = 5.1 correspond to the characteristic signal of protons from the hydroxy groups (-OH). The two triplet signals at δ = 3.8 and 4.3 ppm, characteristic of methylene groups COO-CH_2 and HO-CH_2, corresponded well to the data reported in the literature.[12] As shown, the calculated signal integrals fit very well with the chemical structure of BHET. Furthermore, ^{1}H NMR spectra showed no substantial contribution from impurities, side products, or reaction solvents, indicating that the described procedure was effective for removing impurities from the main glycolysis product.

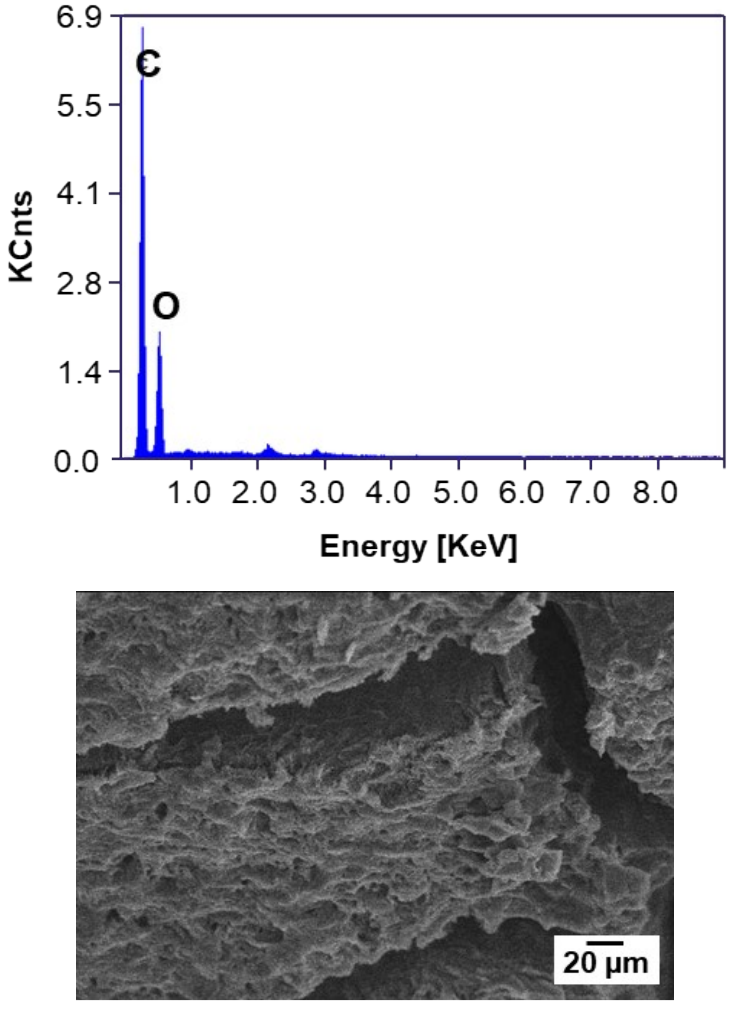

Figure SI 15. EDX spectrum (above) and SEM image (below) of unreacted PET after glycolysis and isolation (catalyst: P([BVMIM]Zn_mCl_n) (**A2,** *R* = 0.75, entry 3, Table 2, Main Manuscript)).

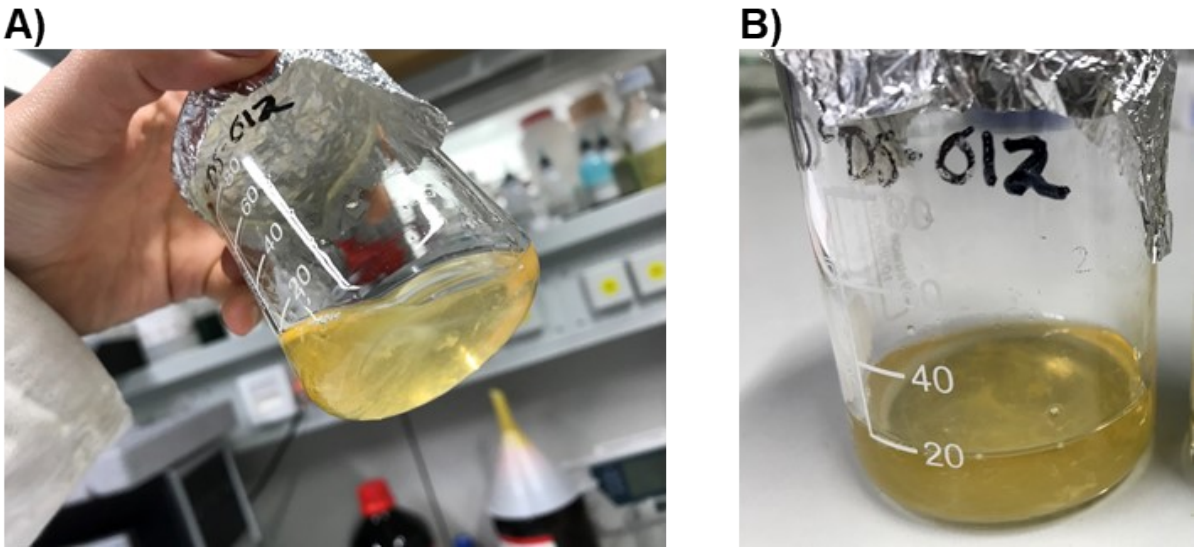

Figure SI 16. Representative images of the resulting solution of P([BVMIM]Zn_mCl_n)/EG after the glycolysis of post-consumer PET and the subsequent crystallization of BHET. After keeping the solution at 4 °C for 24 h, a fine precipitated was visible in the mixture (A). After manipulating the solution at r. t., the precipitate began to dissolve (B).

Table SI 2. Variation of the ^{1}H NMR chemical shifts (DMSO-d_6, δ in ppm) of H_a – H_i in **B1** and its anion exchange derivatives P([BVBIM]Zn_mCl_n) as a function of *R*.

Polymer	H_a	H_b	H_c	H_d	H_e	H_f	H_g	H_h	H_j
B2	0.8	1.2	1.7	4.2	8.0	10.4	5.6	7.5	6.5
B2, *R* = 0.25	0.8	1.2	1.7	4.2	7.9	9.8	5.5	7.5	6.5
B2, *R* = 0.5	0.8	1.2	1.7	4.2	7.8	9.5	5.5	7.3	6.5
B2, *R* = 0.75	0.8	1.2	1.7	4.2	7.8	9.3	5.3	7.3	6.5
B2, *R* = 0.8	0.7	1.1	1.7	4.2	7.7	9.3	5.3	7.2	6.5

Table SI 3. Overview of the properties of P([BVMIM]Zn_mCl_n) (**A2**, *R* = 0.75, Table 2, Main Manuscript) in EG solutions, as a function of concentration, measured by DLS.

Concentration [mg mL^{-1}]	d_h [nm]	PDI
1.0	154.3	0.415
2.0	233.9	0.524
5.0	94.8	0.382
10.0	128.9	0.044

Table SI 4. Overview of the properties of P([BVMIM]Zn_mCl_n) (entries 3 to 6, Table 2, Main Manuscript) in EG solutions, as a function of *R*, measured by DLS.

Entry	*R*	d_h [nm]	PDI
3	0.75	106.2	0.052
4	0.5	94.8	0.207
5	0.25	217.5	0.579
6	0.1	127.6	1.000

References

[1] J.E. Bara, S. Lessmann, C.J. Gabriel, E.S. Hatakeyama, R.D. Noble, D.L. Gin, Synthesis and Performance of Polymerizable Room-Temperature Ionic Liquids as Gas Separation Membranes, Ind. Eng. Chem. Res. 46 (2007) 5397–5404. https://doi.org/10.1021/ie0704492.

[2] J. Estager, P. Nockemann, K.R. Seddon, M. Swadźba-Kwaśny, S. Tyrrell, Validation of Speciation Techniques: A Study of Chlorozincate(II) Ionic Liquids, Inorg. Chem. 50 (2011) 5258–5271. https://doi.org/10.1021/ic200586u.

[3] D. Turk, U. Ghosh, S. Harden, E. Bpt, W. Radke, H. Berg, L. Miles, E. Hughes, M. International, Tips & Tricks: Trouble Analyzing PEGs?, Column. 14 (2022) 18–21–18–21. https://doi.org/10.56530/LCGC.NA.YG3486M1.

[4] B. Chong, G. Moad, E. Rizzardo, M. Skidmore, S.H. Thang, Thermolysis of RAFT-Synthesized Poly(Methyl Methacrylate), (2006). https://doi.org/10.1071/CH06229.

[5] S.L. Simon, Temperature-modulated differential scanning calorimetry: theory and application, Thermochim. Acta. 374 (2001) 55–71. https://doi.org/10.1016/S0040-6031(01)00493-2.

[6] N. Guigo, N. Sbirrazzuoli, Thermal Analysis of Biobased Polymers and Composites, in: 2018: pp. 399–429. https://doi.org/10.1016/B978-0-444-64062-8.00002-4.

[7] R. Urbani, F. Sussich, S. Prejac, A. Cesàro, Enthalpy relaxation and glass transition behaviour of sucrose by static and dynamic DSC, Thermochim. Acta. 304–305 (1997) 359–367. https://doi.org/10.1016/S0040-6031(97)00094-4.

[8] M. Lappalainen, M. Karppinen, Techniques of differential scanning calorimetry for quantification of low contents of amorphous phases, J. Therm. Anal. Calorim. 102 (2010) 171–180. https://doi.org/10.1007/S10973-010-0817-6/TABLES/2.

[9] J.C. Peacock, B.L.D. Peacock, Some observations the dissolving of zinc chloride and several suggested solvents, J. Am. Pharm. Assoc. 7 (1918) 689–697. https://doi.org/10.1002/JPS.3080070807.

[10] F. Neumaier, S. Alpdogan, J. Hescheler, T. Schneider, A practical guide to the preparation and use of metal ion-buffered systems for physiological research, Acta Physiol. 222 (2018) e12988. https://doi.org/10.1111/apha.12988.

[11] Q.F. Yue, C.X. Wang, L.N. Zhang, Y. Ni, Y.X. Jin, Glycolysis of poly(ethylene terephthalate) (PET) using basic ionic liquids as catalysts, Polym. Degrad. Stab. 96 (2011) 399–403. https://doi.org/10.1016/j.polymdegradstab.2010.12.020.

[12] M. Ghaemy, K. Mossaddegh, Depolymerisation of poly(ethylene terephthalate) fibre wastes using ethylene glycol, Polym. Degrad. Stab. 90 (2005) 570–576. https://doi.org/10.1016/j.polymdegradstab.2005.03.011.